

# Baryon masses with improved staggered quarks

**C. Bernard<sup>a</sup>, C. Davies<sup>b</sup>, C. DeTar<sup>c</sup>, Steven Gottlieb<sup>d</sup>, U.M. Heller<sup>e</sup>, J.E. Hetrick<sup>f</sup>,  
L. Levkova<sup>c</sup>, J. Osborn<sup>g</sup>, D.B. Renner<sup>h</sup>, R. Sugar<sup>i</sup> and D. Toussaint<sup>\*h</sup>**

*a* Physics Department, Washington University, St. Louis, MO 63130, USA

*b* Physics Department, Glasgow University, Glasgow, G12 8QQ, UK

*c* Physics Department, University of Utah, Salt Lake City, UT 84112, USA

*d* Physics Department, Indiana University, Bloomington, IN 47405, USA

*e* American Physical Society, One Research Road, Ridge, NY 11961-9000, USA

*f* Physics Department, Pacific University, Stockton, CA 95211, USA

*g* Physics Department, Boston University, Boston, MA 02215, USA

*h* Physics Department, University of Arizona, Tucson, AZ 85721, USA

*i* Physics Department, University of California, Santa Barbara, CA 93106, USA

E-mail: cb@wuphys.wustl.edu, c.davies@physics.gla.ac.uk,  
detar@physics.utah.edu, sg@indiana.edu, heller@aps.org,  
jhetrick@uop.edu, ludmila@physics.utah.edu, josborn@physics.bu.edu,  
dru@physics.arizona.edu, sugar@physics.ucsb.edu,  
doug@physics.arizona.edu

The MILC collaboration's simulations with improved staggered quarks are being extended with runs at a lattice spacing of 0.06 fm with quark masses down to one tenth the strange quark mass. We give a brief introduction to these new simulations and the determination of the lattice spacing. Then we combine these new runs with older results to study the masses of the nucleon and the  $\Omega^-$  in the continuum and chiral limits.

*The XXV International Symposium on Lattice Field Theory  
July 30 - August 4 2007  
Regensburg, Germany*

---

\*Presenter.

## 1. Introduction

In this work we update our determination of the lattice spacing in the MILC collaboration's program of QCD simulations using  $N_f = 2 + 1$  flavors of dynamical staggered quarks with the  $a_{\text{lad}}^2$  action[1], and update our calculations of the nucleon and  $\Omega^-$  masses. Determining the lattice spacing is central to any simulation program. We emphasize that the same lattice spacing determination, with the same uncertainties, affects everything computed from these lattices. The spectrum of the light quark hadrons is an important test of a lattice QCD simulation, and is a standard part of all large lattice QCD programs. Getting these well known masses right gives us confidence in our ability to predict unknown masses and matrix elements. Both the nucleon and  $\Omega^-$  are stable against strong decays and well known experimentally, and hence are good tests of our program. Our previously published work on the light quark spectrum and lattice spacing determination is in Refs. [2, 3].

We are now doing simulations with a smaller lattice spacing,  $a \approx 0.06$  fm, in addition to lengthening some runs and adding runs at other quark masses at larger lattice spacing. The runs at  $a \approx 0.06$  fm are all still in progress, so all results reported here are preliminary. Table I shows the simulation parameters for the  $a \approx 0.06$  fm runs.

$am_q / am_s$	$10/g^2$	size	volume	number	$a$ (fm)	Algorithm
0.0072 / 0.018	7.48	$48^3 \times 144$	$(2.9 \text{ fm})^3$	555	0.060	R
0.0036 / 0.018	7.47	$48^3 \times 144$	$(2.9 \text{ fm})^3$	480	0.060	RHMD-1
0.0018 / 0.018	7.46	$64^3 \times 144$	$(3.8 \text{ fm})^3$	46	0.061	RHMD-4

**Table 1:** Lattice parameters. Lattice spacings come from the smoothed  $r_1/a$  values and  $r_1 = 0.318$  fm. “RHMD- $n$ ” is a RHMD algorithm using  $n$  pseudofermion fields. Details of the algorithms will be given elsewhere.

## 2. Finding the lattice spacing

The results of a lattice computation are in units of the lattice spacing  $a$ , so a determination of  $a$  in physical units is essential. This requires taking some physical quantity (or average over quantities) as a standard. At this time we are using the  $\Upsilon$  mass splittings determined by the HPQCD group[4]. A possible alternative is  $f_\pi$ , and we are investigating whether this would be better[5]. Because  $\Upsilon$  mass splittings are not available on all of our ensembles and because the static quark potential can be accurately determined, we use  $r_1$  defined by  $r_1^2 F(r_1) = 1.0$  [6, 7] as a quantity to interpolate the lattice spacing, as described in Ref. [3]. Thus, the  $\Upsilon$  splittings give  $r_1 = 0.318(7)$  fm, which is then used to determine the lattice spacing for all gauge couplings and quark masses.

Static quark potentials were calculated from correlators of time direction lines, with Coulomb gauge fixing for the spatial connections[7]. As the lattice spacing decreases, determining the static potential becomes more difficult because of the increasing constant term, corresponding to the singular self-energy of the static quark. Since the Wilson loop expectation value falls off exponentially as  $\langle W(R, T) \rangle \approx \exp(-V(R)T)$ , a larger constant in  $V(R)$  translates into an exponentially smaller

expectation value of  $W(R, T)$ , and larger fractional statistical error. This can be alleviated, at the cost of some spatial resolution, by smearing the time direction links in the lattice.

Figure 1a shows the static quark potential, with and without one iteration of APE smearing of the time direction links, while Fig. 1b shows the static quark potential at  $m_q = 0.4m_s$  for four different lattice spacings.

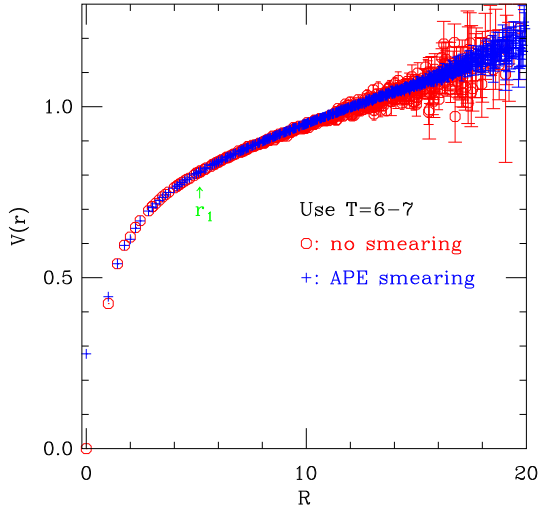


Figure 1a: The static quark potential, with and without APE smearing of the time direction links. This is for the  $am_q/am_s = 0.0072/0.018$  run. The constants in the potential differ (that’s the point), so we added 0.27731 to the smeared potential to show the agreement. (This shift forces the potentials to agree at  $r_1$ .)

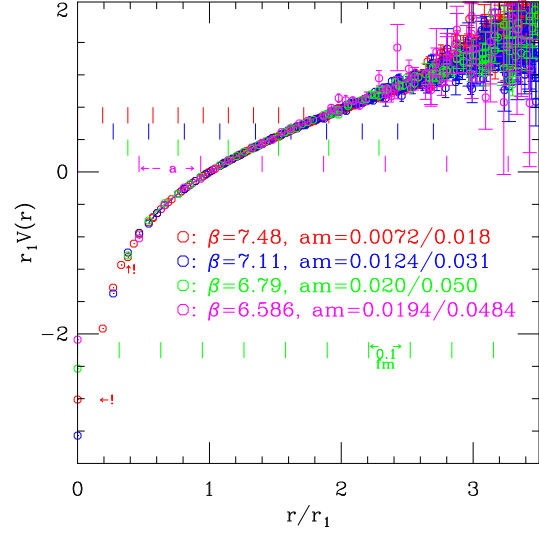


Figure 1b: The static quark potential at  $m_q = 0.4m_s$  for four different lattice spacings, roughly  $a = 0.06, 0.09, 0.125$  and  $0.15$  fm. The  $a = 0.06$  fm potential uses smearing of the time links. The colored rulers near  $V = 0$  are in units of the corresponding lattice spacings, while the “physical” ruler near  $V = -2$  is in units of  $0.1$  fm.

In Fig. 2b note the visible lattice artifact at the on-axis  $(2, 0, 0)$  point marked with  $\uparrow!$ . The spatial range used for the  $r_1$  determination at  $a \approx 0.06$  fm was  $4.01$  to  $7.01$ . Also note that the  $a = 0.06$  fm potential (red) at  $r = 0$  (marked with  $\leftarrow!$ ) is much smaller in magnitude than if it continued the trend, again showing the effect of the smearing.

To find  $r_1$  the potential was fit to  $V(r) = C + A/r + Br$  for a range around  $r_1$ . With  $a \approx 0.06$  fm, lattice artifacts are unimportant in these distance ranges. Errors are from a jackknife analysis, using a block size of 20 lattices, or 100 molecular dynamics time units. Figure 2a shows estimates of  $r_1/a$  from various spatial and temporal distance ranges without smearing, while Fig. 2b (right half) shows fits with one iteration of APE smearing, including projection onto  $SU(3)$ . The fits shown in Figs. 2a and 2b (right) are from fitting the “Wilson loops” to a single exponential:  $V(r) = \log(W(r, T)/W(r, T+1))$ . We also do fits including an excited state of the potential. This gives less dependence on fit range (smaller systematic error) but larger statistical errors. The  $r_1/a$  estimates on the left side of Fig. 2b are from such two-state fits. Fitting this, together with our previous results at  $a \approx 0.018, 0.015, 0.0125$  and  $0.09$  fm, we get a “smoothed  $r_1$ ”, which is then used to set

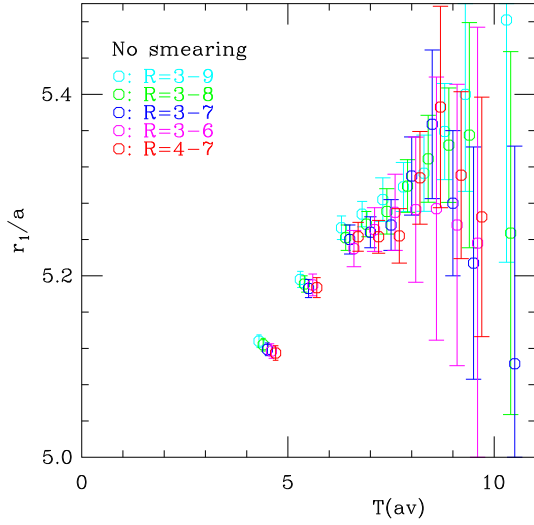


Figure 2a: Estimates of  $r_1/a$  from “loops” with unsmeared time links. This is for the  $am_q/am_s = 0.0072/0.018$  run.

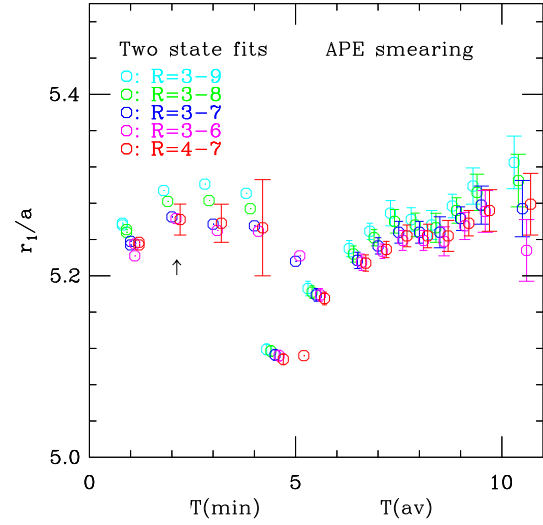


Figure 2b: Estimates of  $r_1/a$  from the same run, with one iteration of APE smearing including projection onto SU(3) for the time direction links (right side). Fits including an excited state (left side). The arrow indicates the point taken as our estimate.

the length scale for all ensembles.

### 3. Nucleon and $\Omega^-$ masses

Both the nucleon and the  $\Omega^-$  are stable against strong decays, and so their masses should be accessible in a straightforward way to lattice calculations. In principle the nucleon mass could be used to determine the lattice spacing. In practice its correlators are noisy, and the non-trivial chiral extrapolation makes an accurate determination difficult. The  $\Omega^-$  has a very mild chiral extrapolation — no terms with  $\log(m_\pi)$  or  $m_\pi^3$  at one loop order. Since it contains three valence strange quarks, its mass is very sensitive to the strange quark mass. Therefore, the  $\Omega^-$  mass checks our determination of the lattice strange quark mass from pseudoscalar physics.

Figure 3a shows the nucleon correlators from the  $a \approx 0.06$  fm runs at  $0.4m_s$  and  $0.2m_s$ . Note the expected difference in the slope, the alternating (opposite parity) signal at short distances, and the increasing error bars at large distances. Figure 3b shows fits to one of these correlators ( $m_q \approx 0.2m_s$ ) as well as correlators for roughly the same light quark mass at  $a \approx 0.125$  and  $0.09$  fm. In this plot the size of the symbol is proportional to the confidence level of the fit, with the symbol size used in the captions corresponding to 50%. From graphs like this we look for a plateau and reasonable confidence level ( $\chi^2$ ). The arrows in the graph indicate the fits that were chosen. Most of the difference in the masses comes from the fact that the light quark masses in these three runs were not exactly equivalent, and some comes from effects of lattice discreteness.

In Figure 4a we show nucleon masses for  $a \approx 0.0125$  fm,  $0.09$  fm and  $0.06$  fm, where the three colored arrows in Fig. 3b indicate the fits that were chosen to include in this figure. The black

error bar at the left is the experimental value. The error on this comes from the uncertainty in  $r_1$  (We use 0.318(7) fm). Another point at  $a \approx 0.06$  fm at  $m_l \approx 0.1m_s$  ( $(m_\pi r_1)^2 \approx 0.12$ ) is in progress.

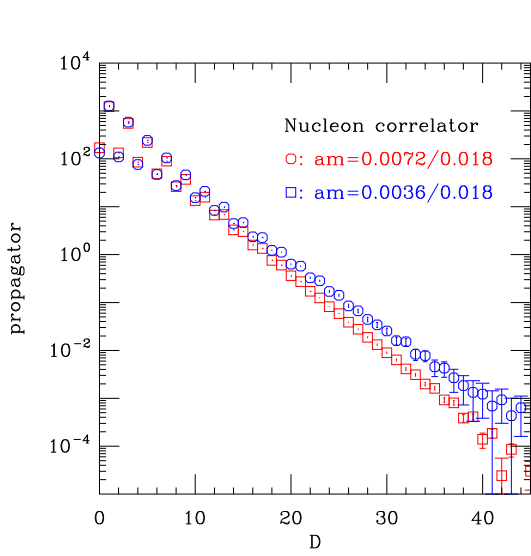


Figure 3a: Nucleon correlators at  $a = 0.06$  fm for light quark masses  $0.4m_s$  and  $0.2m_s$ .

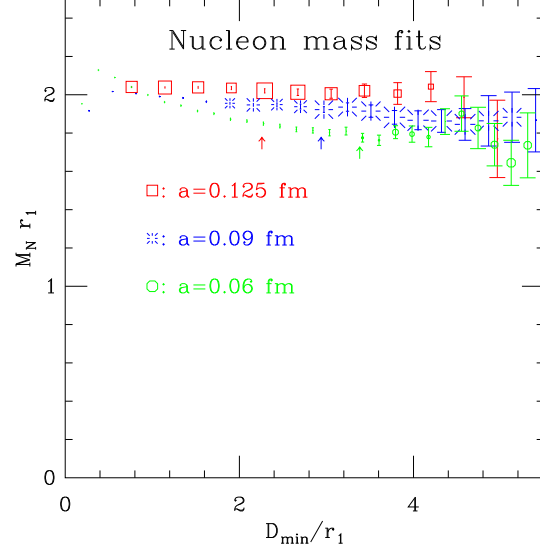


Figure 3b: Nucleon mass fits for  $m_l = 0.2m_s$ .

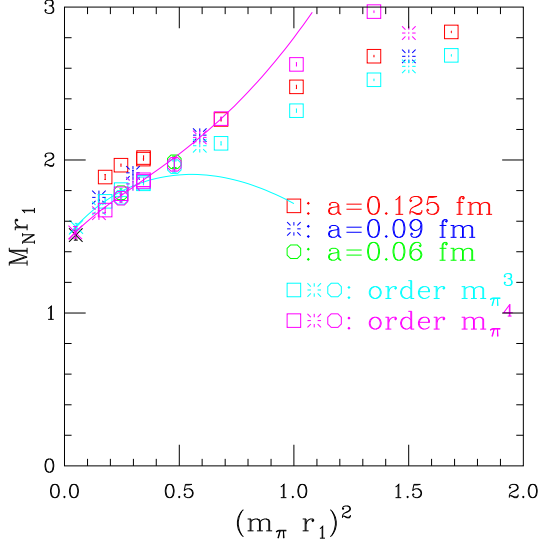


Figure 4a: Nucleon masses (red blue and green symbols), and fits to the nucleon mass (cyan and magenta).

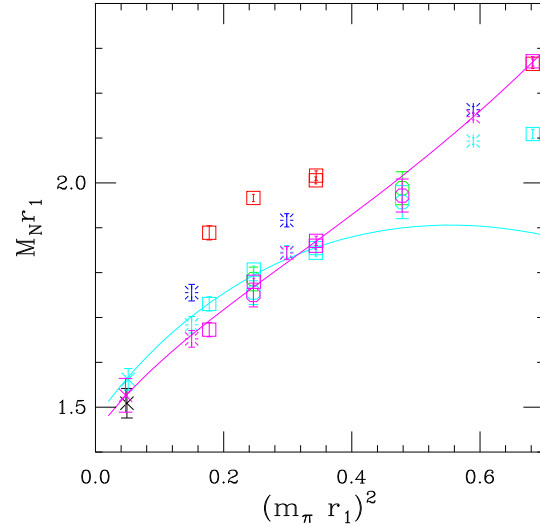


Figure 4b: The same, expanded to show the small quark mass region. The points with  $m_l = 0.2m_s$  are from the fits indicated with arrows in Fig. 3b.

We show two forms for extrapolating the nucleon mass to the physical quark mass and continuum limit. The first (cyan) includes only the lowest order nonanalytic correction, order  $m_\pi^3$ .

$$m_N r_1 = M_0 r_1 + A_1 (m_\pi r_1)^2 + B_1 a^2 \alpha + r_1 \frac{-3g_A^2}{32\pi f_\pi^2} m_\pi^3 \quad (3.1)$$

In these fits we just set  $f_\pi$ ,  $g_A$  and  $M_\Delta - M_N$  to their physical values. The cyan and magenta symbols in Figs. 4a and 4b are the data points with the fitted lattice spacing corrections,  $B_1 a^2 \alpha$ , subtracted, *i.e.* at  $a = 0$ , and the cyan and magenta lines are the fitting function at  $a = 0$ .

The second form (magenta)[8] includes the  $\Delta$  without the assumption that  $\Delta = M_\Delta - M_N \gg f_\pi$ . When Taylor expanded in powers of  $m_\pi$  this includes terms up to  $m_\pi^4$ ,  $m_\pi^4 \log(m_\pi)$ .

$$m_N r_1 = M_0 r_1 + A_1 (m_\pi r_1)^2 + A_2 (m_\pi r_1)^4 + B_1 a^2 \alpha + B_2 (m_\pi r_1)^2 a^2 \alpha + r_1 \frac{6g_A^2}{25\pi^2 f_\pi^2} H(m_\pi, M_\Delta - M_N, \Lambda) \quad (3.2)$$

where, if  $m_\pi < \Delta = M_\Delta - M_N$

$$H(m_\pi, \Delta, \Lambda) = \Delta^3 \log(2\Delta/m_\pi) + \Delta m_\pi^2 \left( \frac{3}{2} \log(m_\pi/\Lambda) - 1 \right) - (\Delta^2 - m_\pi^2)^{3/2} \log \left( \Delta/m_\pi + \sqrt{\Delta^2/m_\pi^2 - 1} \right) - \Delta m_\pi^2 \left( \frac{3}{2} \log(2\Delta/\Lambda) - \frac{3}{4} \right) \quad (3.3)$$

if  $m_\pi > \Delta$

$$H(m_\pi, \Delta, \Lambda) = \Delta^3 \log(2\Delta/m_\pi) + \Delta m_\pi^2 \left( \frac{3}{2} \log(m_\pi/\Lambda) - 1 \right) - (m_\pi^2 - \Delta^2)^{3/2} \arccos(\Delta/m_\pi) - \Delta m_\pi^2 \left( \frac{3}{2} \log(2\Delta/\Lambda) - \frac{3}{4} \right) \quad (3.4)$$

Systematic errors have not been properly analyzed yet, and the data set is incomplete. With these reservations, the order  $m_\pi^4$  chiral fit in Fig. 4 at the physical quark mass is  $M_N r_1 = 1.52 \pm .04 \pm \text{syst.}$ , or  $M_N(\text{MeV}) = 942 \pm 25 \pm \text{syst.}$ , where systematic errors on  $M_N r_1$  must be at least 0.045, the difference between the two chiral fitting forms. We are also experimenting with chiral extrapolations using fitting forms from partially quenched staggered chiral perturbation theory[9].

In fitting the  $\Omega^-$  mass the chiral extrapolation is simpler, but we must deal with its dependence on the strange quark mass. Our lattice simulations were run with an estimate of the strange quark mass and only after running the simulation can we determine what the correct strange quark mass is. Thus, we compute correlators at two valence strange quark masses, and then interpolate to the valence strange quark mass determined from pseudoscalar mesons (basically  $M_K$ ). Figure 5a (like figure 3b for the nucleon) shows fits to the  $\Omega^-$  correlators for runs at three different lattice spacings with  $m_l \approx 0.2m_s$ , again with arrows indicating the fit we chose. For the chiral and continuum extrapolation we use a linear extrapolation in  $am_l$  and  $a^2 \alpha$ , which fits well with  $\chi^2/\text{dof} = 6.0/7$ .

$$M_{\Omega} r_1 = M_0 r_1 + A(m_\pi r_1)^2 + B a^2 \alpha \quad (3.5)$$

Figure 5b shows the  $\Omega^-$  masses interpolated to the strange quark mass determined from pseudoscalar mesons as a function of light quark mass. It also shows the fit form above for  $a \approx 0.125$ , 0.09 and 0.06 fm, and in the continuum limit, *i.e.* with  $B$  set to zero. The black symbol is the experimental value for  $m_{\Omega} r_1$ , where the error is from the uncertainty in  $r_1$ .

Errors on the extrapolated lattice result are statistical (0.7%), determination of  $m_s$  from pseudoscalars (0.6%), and an estimate of neglected NNLO terms in chiral extrapolation ( $_{0.05}^0$ ). Other small errors come from using the wrong strange sea quark mass, and the choice of procedure for

fixing strange quark mass. Using data available at conference time, the continuum and chiral extrapolated value is  $M_\Omega * r_1 = 2.679^{+0.025}_{-0.056}$ . Converting to physical units using  $r_1 = 0.318(7)$  and adding errors, this is  $M_\Omega(\text{MeV}) = 1660^{+40}_{-50}$ , where the experimental value is 1672 MeV.

This work is supported by the US Department of Energy and National Science Foundation. Computations were done at the NSF Teragrid, NERSC, USQCD centers and computer centers at the Universities of Arizona, Indiana, Utah and California at Santa Barbara.

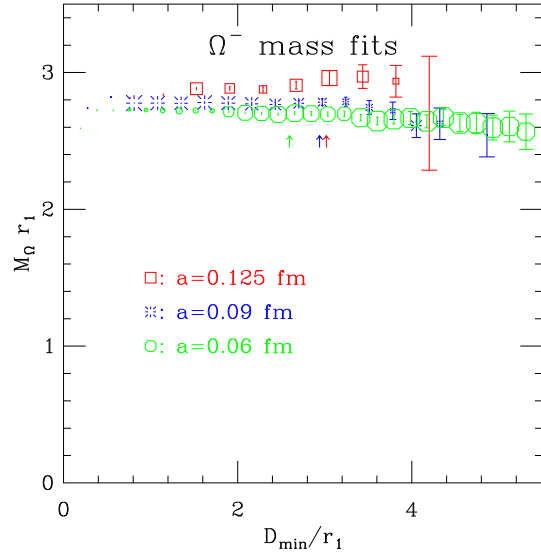


Figure 5a:  $\Omega^-$  mass fits for  $m_l = 0.2m_s$ . In these plots the strange quark mass has not been tuned to the correct  $m_s$ ; it is one of the masses at which correlators were computed.

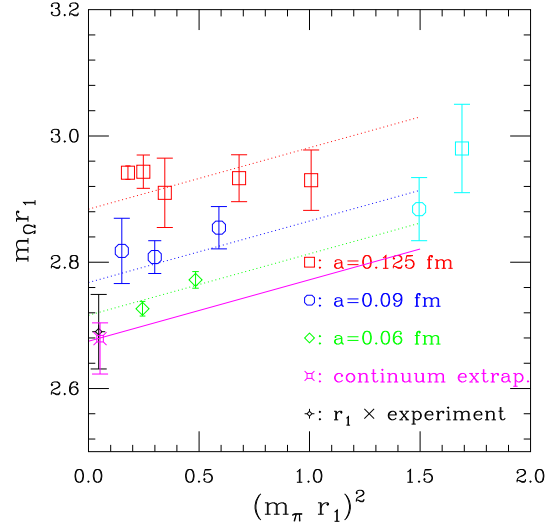


Figure 5b:  $\Omega^-$  masses and fitting (see text). The error on the experimental point is from the error in  $r_1$ .

## References

- [1] T. Blum *et. al* [MILC], Phys. Rev. D **55**, 1133 (1997); K. Orginos and D. Toussaint, Phys. Rev. D **59** (1999) 014501; K. Orginos, D. Toussaint and R.L. Sugar, Phys. Rev. D **60** (1999) 054503; G.P. Lepage, Phys. Rev. D **59** (1999) 074502; J.F. Lag  e and D.K. Sinclair, Nucl. Phys. (Proc. Suppl.) **63**, 892 (1998); C. Bernard *et. al* [MILC], Phys. Rev. D **58** (1998) 014503.
- [2] Claude Bernard *et. al* [MILC], Phys. Rev. D **64** (2001) 054506 [hep-lat/0104002].
- [3] C. Aubin *et. al* [MILC], Phys. Rev. D **70** (2004) 094505. [hep-lat/0402030]
- [4] C. Davies and G.P. Lepage, HPQCD collaboration, private communication; M. Wingate *et al.*, Phys. Rev. Lett. **92** (2004) 162001 [hep-ph/0311130]; A. Gray *et al.*, Phys.Rev. D **72** (2005) 094507 [hep-lat/0507013].
- [5] Poster by C. Bernard [MILC], this conference.
- [6] R. Sommer, Nucl. Phys. **B411**, 839 (1994).
- [7] C. Bernard *et. al* [MILC], Phys. Rev. D **62**, 034503 (2000) [hep-lat/0002028].
- [8] E. Jenkins, Nucl. Phys. B **368**, 190 (1992); V. Bernard, N. Kaiser and U.G. Meissner, Z. Phys. **C60**, 111 (1993).
- [9] J. Bailey, Phys. Rev. D **75** 114505 (2007) [hep-lat/0611023].